Impact of aerial and ground users coexistence on user-centric D-MIMO networks

Wilker de O. Feitosa, Igor M. Guerreiro, Fco. Rodrigo P. Cavalcanti, and Maria Clara R. Lobão

***Abstract*— Distributed multiple-input multiple-output (D-MIMO) is a promising network technology for 5G-beyond systems due to their capability of providing better coverage and more reliable communication. In this context, several access points with small antenna arrays are spread over the coverage area to perform joint coherent transmission, possibly with user-centric clustering strategies, different from conventional cellular massive multiple input multiple output (MIMO) technology comprising fewer base stations equipped with large antenna arrays. Besides, uncrewed aerial vehicles (UAVs) are mobile devices with increasing demand in the context of 5G-beyond systems, and due to their 3D mobility, they represent a challenge in terms of network resource and interference management. Thus, this work presents a resource allocation analysis of a D-MIMO network in which UAVs and ground UEs (GUEs) coexist. Some network parameters are varied and their impact are studied, such as clustering approach, use of orthogonal bands and UAV load. Simulation results indicate that UAV coexistence with GUEs in general does not decrease the network performance beyond what would be expected by an equal load of GUEs in typical propagation conditions. In the considered scenario, adding UAVs deteriorates 65% less than adding the equal amount of GUEs.**

***Keywords*— distributed MIMO, UAV, interference, clustering.**

I. Introduction

As the fifth generation (5G) systems implementation grows in popularity around the world, the demand for higher speed commmunications, larger coverage, diversified use cases and reliable connection increase at even faster pace [1]. This leaves an important responsibility for the beyond fifth generation (B5G) and sixth generation (6G) systems. To tackle those demands a series of technologies and architectures are being proposed [2]. In this context, the distributed multiple-input multiple-output (D-MIMO) technology arises with the promise of more uniform quality of service (QoS), high data rates and increased interference handling capabilities [3], [4].

The D-MIMO networks consist of a large number of access points (APs) with few antennas per AP over a relatively small coverage area. The APs in a D-MIMO network operate in a highly cooperative manner, and to ensure the network scalability and feasibility those APs tend to form clusters for serving users/groups of users [5].

This work was supported in part by Ericsson Research, Technical Cooperation Contract UFC.50, by the Brazilian National Council for Scientific and Technological Development (CNPq) Proc. no. 303625/2022-8, by FUNCAP/Universal Grant no. UNI-0210-00043.01.00/23.

Wilker de O. Feitosa, Igor M. Guerreiro, Fco. Rodrigo P. Cavalcanti and Maria Clara R. Lobão are with the Wireless Telecommunications Research Group (GTEL), Federal University of Ceará (UFC), Fortaleza, Brazil. E-mails: {wilker, igor, rodrigo, clara}@gtel.ufc.br.

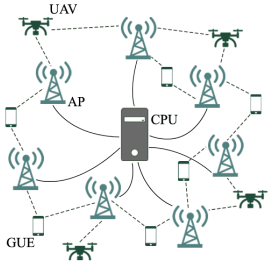

Fig. 1. Illustration of a D-MIMO network serving different types of UEs.

The uncrewed aerial vehicles (UAVs), with their aerial mobility capability, are a type of user equipment (UE) already considered in legacy networks [6] and envisioned to be in significant demand by the time of 6G deployment. Their channel propagation properties are different from the ones usually observed in ground user equipments (GUEs), and thus their presence in mobile networks demands attention due to new interference and mobility patterns [6], [7].

The contribution of this work is thus the investigation of the co-existence of UAVs and GUEs in a D-MIMO network. More precisely, different case studies are described towards the evaluation the the impact of adding aerial UEs on: i) The per-UE SE; ii) The resource allocation policy; iii) The user-centric clustering strategy typically adopted for GUEs. The key findings of this work are two fold: UAV coexistence in D-MIMO does not lead to spectral efficiency (SE) degradation, and the clustering formation algorithm tends to have different behaviors for the UAVs and GUEs. This and other results shown in the rest of this paper help to enlighten the radio resource allocation policy a network operator has to face when managing a network under aerial UE load.

II. System Model

Consider the uplink of a D-MIMO network consisting of L APs, each equipped with S uniform linear arrays (ULAs) of N antenna elements each, and K single-antenna UEs. The system operates on time division duplex (TDD) mode.

The UEs are split into two groups: K_{UAV} aerial UEs, or simply UAVs, and K_{GUE} ground-based users or simply GUEs, so that $K = K_{\text{UAV}} + K_{\text{GUE}}$. Moreover, the APs are considered to have an ideal fronthaul with a central processing unit (CPU). Figure 1 illustrates the considered D-MIMO network.

A. User-centric cluster strategy

This work assumes the formation of user-centric clusters, i.e., each UE can be connected to multiple APs depending on

its channel gain. The dynamic cooperation clustering (DCC) concept for user-centric D-MIMO is an adaptation of the well-known Coordinated Multi-Point (CoMP) interference mitigation framework [8]. For each user, the cell-free DCC basically:

1) sets the AP with the best channel gain as the master AP;
2) assigns other APs that serve only users with orthogonal pilots and that are within a channel gain *threshold* range.

As benchmark, UEs can be connected to *all APs* within the coverage area, although this is shown not to be scalable [5].

B. Propagation Model

The radio link between a UE transmitter and an AP receiver is considered to follow a Rician Single Input Multiple Output (SIMO) channel model, in which the Rayleigh components are correlated. The propagation channel $\mathbf{h}_{k,l,s} \in \mathbb{C}^N$ between user k and the array s at the AP l is defined as:

$$\mathbf{h}_{k,l,s} = \left[\sqrt{\frac{\bar{K}_{k,l}}{\bar{K}_{k,l}+1}} \mathbf{a}_{k,l,s} + \sqrt{\frac{1}{\bar{K}_{k,l}+1}} \mathbf{h}^{(w)}_{k,l,s} \right] \sqrt{\beta_{k,l,s}}\,, \tag{1}$$

where $\bar{K}_{k,l}$ is the Rician K-factor, $\mathbf{a}_{k,l,s} \in \mathbb{C}^N$ is the array steering vector, $\mathbf{h}^{(w)}_{k,l,s} \sim \mathcal{N}(0, \mathbf{R}_{k,l,s})$ is the correlated Rayleigh fading component, $\mathbf{R}_{k,l,s} \in \mathbb{C}^{N\times N}$ is the channel correlation matrix as in [9]. Finally, $\beta_{k,l,s}$ is the large-scale coefficient defined as:

$$\beta_{k,l,s} = 10^{\frac{PL_{k,l}+SH_{k,l}+G_{k,l,s}}{10}}\,, \tag{2}$$

in which $PL_{k,l}$ is the path-gain, $SH_{k,l}$ is the correlated shadow fading with standard deviation of σ_{SH}, and $G_{k,l,s}$ is the antenna gain. Note that these three large-scale parameters are in dB scale.

The large-scale parameters and the Rician K-factor depend on the line-of-sight (LoS) state and are modeled as in [10] for GUEs, and as in [11] for UAVs, considering an urban micro (UMi) scenario for both UE groups.

C. Antenna Modelling

The AP's antennas are directional with radiation pattern as described in [12]. Thus, to obtain 360° coverage, the APs are three-sectorized, meaning that their $S = 3$ ULAs' maximum gain in azimuth domain are spaced 120° from each other.

The steering vectors that compose the channel in (1) are defined as follows:

$$\mathbf{a}_{k,l,s} = \left[u^1_{k,l,s} \dots u^M_{k,l,s}\right]^T\,, \tag{3}$$

$$u^m_{k,l,s} = e^{j\frac{2\pi}{\lambda}(m-1)d\sin\theta_{k,l,s}\cos\gamma_{k,l,s}}\,, \tag{4}$$

where d is the antenna spacing, $\theta_{k,l,s}$ and $\gamma_{k,l,s}$ are the Angle of Arrival (AoA) in elevation and azimuth domains, respectively. The arrays are considered to be tilted by θ_{tilt} radians.

The antenna gain in (2) is drawn from the 3D gain function G_A from [12], so that $G_{k,l,s} = G_A(\theta_{k,l,s}, \gamma_{k,l,s}, \theta_{\text{tilt}})$, representing the antenna pattern per element, which can be calculated based on the following definitions:

$$G_E(\theta, \gamma, \theta_{\text{tilt}}) = -\min\left[-\left(G_V(\theta, \theta_{\text{tilt}}) + G_H(\gamma)\right), A_m\right]\,, \tag{5}$$

where $G_V(\theta, \theta_{\text{tilt}})$ and $G_H(\gamma)$, are the vertical and horizontal gain, defined in [12], $\theta_{3\text{dB}} = 15°$ and $\gamma_{3\text{dB}} = 70°$ are the vertical and horizontal half power beamwidth (HPBW) angle and $A_m = 20$ dB is the maximum antenna attenuation.

D. Channel Estimation

A pilot-assisted channel estimation procedure is assumed in this work. There are $\tau_p = K$ orthogonal pilot signals $\phi_1, \dots, \phi_{\tau_p}$ of length τ_p with $||\phi_t||^2 = \tau_p$, so no pilot contamination is considered. Similar to [3], the signal received at the AP is cross-correlated with the normalized pilot sequence transmitted by the UEs, so the resulting signal at the AP is:

$$\mathbf{z}_{t_k,l,s} = \sum_{i\in\mathcal{P}_k} \sqrt{p_i\tau_p}\mathbf{h}_{i,l,s} + \mathbf{n}_{t_k,l,s}\,, \tag{6}$$

where $\mathbf{z}_{t_k,l,s}$ is the signal received at the AP l in the array s arriving from user k using the pilot t_k; p_i is the transmitted power from UE i; $\mathbf{h}_{i,l,s}$ is the channel between UE i and the AP l in the array s; $\mathbf{n}_{t_k,l,s} \sim \mathcal{N}(0, \sigma^2\mathbf{I}_N)$ is the noise at the receiver and finally $\mathcal{P}_k$ is the subset of UEs that use the same pilot, which in this case has always cardinality one.

The channel estimate $\hat{\mathbf{h}}_{k,l,s}$ is then obtained by applying a minimum mean square error (MMSE) estimator, yielding:

$$\hat{\mathbf{h}}_{k,l,s} = \sqrt{p_k\tau_p}\mathbf{R}_{k,l,s}\boldsymbol{\Psi}^{-1}_{t_k,l,s}\mathbf{z}_{t_k,l,s}\,, \tag{7}$$

where $\boldsymbol{\Psi}_{t_k,l,s} = \mathbb{E}\{\mathbf{z}_{t_k,l,s}\mathbf{z}^H_{t_k,l,s}\}$ is the correlation matrix of the signal in (6), and $\mathbf{R}_{k,l,s}$ denotes the correlation matrix of channel $\mathbf{h}_{k,l,s}$ in (1).

E. Receiver Processing and SE

The SE will be used as a Key Performance Indicator (KPI) in this work. The channel estimation process described above will be performed by the AP and then sent to the CPU along with the local signal estimate for the final decoding. The uplink complex baseband signal $\mathbf{y}_{l,s} \in \mathcal{C}^N$ received by the AP l at the array s is given by:

$$\mathbf{y}_{l,s} = \sum_{k=1}^{K} \mathbf{h}_{k,l,s}s_k + \mathbf{n}_{l,s}\,, \tag{8}$$

where s_i is the symbol transmitted by the UE i and $\mathbf{n}_{l,s} \sim \mathcal{N}_{\mathcal{C}}(0, \sigma^2\mathbf{I}_N)$. Now let $\mathbf{v}_{k,l,s}$ be the combining vector used by the AP l at the array s to locally estimate the symbol s_k from user k. In this work, the local MMSE (L-MMSE) combiner will be used, as according to [13], it is the combiner that maximizes the SE when only local data is used:

$$\mathbf{v}_{k,l,s} = p_k\left(\sum_{i=1}^{K} p_i\left(\hat{\mathbf{h}}_{i,l,s}\hat{\mathbf{h}}^H_{i,l,s} + \mathbf{C}_{i,l,s}\right) + \sigma^2\mathbf{I}_N\right)^{-1}\mathbf{D}_{k,l,s}\hat{\mathbf{h}}_{k,l,s}\,, \tag{9}$$

where $\mathbf{C}_k = \text{diag}(\mathbf{C}_{k,1,1}, \dots, \mathbf{C}_{k,L,S})$; $\mathbf{C}_{k,l,s} = \mathbb{E}\{\hat{\mathbf{h}}_{k,l,s}\hat{\mathbf{h}}^H_{k,l,s}\}$ and $\mathbf{D}_{k,l,s}$ is a block-diagonal matrix related to the cluster of arrays that serves the user k [5]. When the local AP estimates arrive at the CPU, the latter linearly decodes its information using large scale fading decoding

(LSFD) [3]. Let $\mathbf{g}_{k,i} = \left[\mathbf{v}_{k,1,s}^H \mathbf{h}_{i,1,s} \dots \mathbf{v}_{k,L,s}^H \mathbf{h}_{i,L,s}\right]$ be the received-combined channels between the UE k and each of the APs. The optimal LSFD weights $\mathbf{w}_k$ for maximizing the signal to interference-plus-noise ratio (SINR) are given by [14]:

$$\mathbf{w}_k = p_k \left(\sum_{i=1}^{K} p_i \mathbb{E}\{\mathbf{g}_{k,i}\mathbf{g}_{k,i}^H\} + \mathbf{F}_k + \tilde{\mathbf{D}}_k \right)^{-1} \mathbb{E}\{\mathbf{g}_{k,k}\}. \tag{10}$$

where for numerical regularization $\tilde{\mathbf{D}}_k \in \mathbb{R}^{LS \times LS}$ is a diagonal matrix whose $d_{l,s}$ is one if the AP l does not serve the user k in the array s and zero otherwise; $\mathbf{F}_k = \text{diag}\left(\mathbb{E}\{||\mathbf{D}_{k,1,1}\mathbf{v}_{k,1,1}||^2\} \dots \mathbb{E}\{||\mathbf{D}_{k,L,S}\mathbf{v}_{k,L,S}||^2\}\right) \in \mathbb{C}^{LS \times LS}$. Using (10), the SINR can be calculated in its simplified form as:

$$\begin{aligned}\text{SINR}_k =& p_k \mathbb{E}\{\mathbf{g}_{k,k}^H\} \Bigg(\sum_{i=1}^{K} p_i \mathbb{E}\{\mathbf{g}_{k,i}\mathbf{g}_{k,i}^H\} \\ &- p_k \mathbb{E}\{\mathbf{g}_{k,k}\}\mathbb{E}\{\mathbf{g}_{k,k}^H\} + \mathbf{F}_k + \tilde{\mathbf{D}}_k \Bigg)^{-1} \mathbb{E}\{\mathbf{g}_{k,k}\}. \end{aligned} \tag{11}$$

The SE in this scenario can be calculated as:

$$\text{SE}_k = \left(1 - \frac{\tau_p}{\tau_c}\right) \log_2\left(1 + \text{SINR}_k\right), \tag{12}$$

in which τ_c is the length of the coherence block and τ_p denotes the duration of the uplink channel estimation phase.

III. Impact of aerial UE coexistence: Case studies

In this section three case studies related to the aerial and ground UEs coexistence in D-MIMO networks are described. The goal is to evaluate the impact of adding aerial UEs on: i) The per-UE SE; ii) The resource allocation policy; iii) The user-centric clustering strategy typically adopted for GUEs.

The D-MIMO network described in Section II is assumed to be configured as if all UEs are ground ones, then impacting both antenna and signal processing configuration at both ends. Numerical evaluation will be presented and discussed in Section IV.

A. Case study 1: SE evaluation under aerial UE load

In this case study, all APs are available to serve the UEs, i.e., no clustering is configured. Aerial UEs coexist with ground ones, i.e., both UE types share the same resources. Under such a network setup, the service provider needs to assess the impact of adding some aerial UE load in the per-UE SE.

To this end, the per-UE SE is evaluated for a first UE load comprising only GUEs, and compared with the cases when the UE load is twice as high as the first load with:

1) GUEs and aerial UEs with equal proportion.
2) only GUEs.
3) only aerial UEs.

The rationale behind this assessment is to understand whether aerial UEs degrade the system performance in terms of per-UE SE, which may influence service provider decisions related to network optimization.

B. Case study 2: Resource allocation under aerial UE load

This case study can be seen as a follow-up of the previous one. Nevertheless, here the system bandwidth is sliced into equal bandwidth parts (BWPs). Then, each UE category operates on orthogonal separate BWPs.

In this context, the aerial UE coexistence is investigated in a more explicit manner. It is of interest to understand whether any SINR improvement aerial UEs may benefit from can compensate for the explicit bandwidth decrease.

C. Case study 3: Cluster configuration under aerial UE load

In this case study, the well known DCC [5] is evaluated as a means to carry out user-centric AP clustering in the D-MIMO network, as described in Section II-A. The same channel gain threshold is adopted independently of the type of UE, i.e., aerial or ground.

The per-UE SE and the per-UE cluster size are evaluated for different values of the threshold. Here, it is important to understand whether the cluster strategy can be performed with a single channel gain threshold under both aerial and ground UEs. Otherwise, a hybrid approach would be necessary to avoid unnecessary radio resource usage by aerial UEs.

IV. Numerical evaluations

In this section the D-MIMO network described in Section II is simulated for different configurations to obtain numerical evaluations in terms of:

- SE according to (12);
- Link capacity;
- Cluster size.

In the first part of this section, a small network is simulated, in which the impact of the UE load is analyzed. In the second part of this section, a larger scenario is simulated. Then, to cope with scalability, the cell-free DCC is included in the model and its impact on performance is analyzed.

A. Evaluation of Case Study 1

In this subsection, the impact of the presence of UAVs on the SE is investigated. More specifically, the system load is stressed either by adding new UAVs to the network or changing the UAV/GUE proportion. The impact of each UE type on KPIs is also addressed. Notice that UAVs and GUEs share the same radio spectrum resources.

Considering the scenario described in Section II and using the parameters in table I, the Fig. 2 presents SE empirical cumulative distribution functions (ECDFs) for different proportions between UAVs and GUEs. Along this subsection, these curves will be compared in terms of system load or QoS.

For this first analysis, our base scenario is represented by the black curve, which corresponds to the UEs' SE in a system following the parameters on Table I, but with only 5 GUEs using the network's resources. Now let us consider the arrival of new users that will share the same resources as the existing GUEs. Initially, we assume the addition of 5 UAVs in the system, which is represented by the red curves. In this first case, the continous red curve represent the SE ECDF

TABLE I
SMALL NETWORK PARAMETERS.

Parameter	Value
Coverage area	300x300 m
Number of APs	$L = 9$
Number of Sectors per AP	$S = 3$
Number of users	$K = [5, 10]$
UAV percentage	$[0, 50, 100]\%$
Carrier frequency	f_c = 2 GHz
Communication bandwidth	W = 20 MHz
GUE and AP heights	1.5 m, 11.5 m
UAV height	uniform, $[23, 230]$ m
Uplink power per UE	p_k = 100 mW
Antenna spacing	$d = (1/2)\,\lambda$
GUEs σ_{sh} (LoS, NLoS)	4, 8.2 dB
UAVs σ_{sh} (LoS [11], NLoS)	$\max(2, 5e^{h_{\text{UAV}}/100})$, 8 dB
LoS probability model (GUEs,UAVs)	[10],[11]

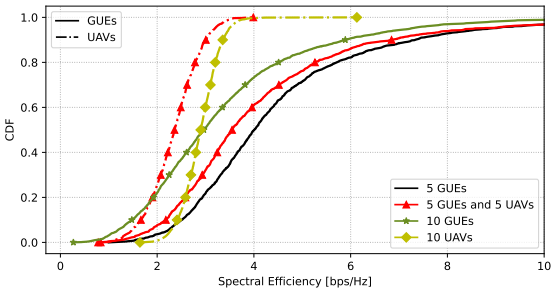

Fig. 2. SE curves for various UE loads.

of the GUEs affected by the arrival of the UAVs and the dotted red curve represent the ECDF of the UAVs in the system. For the case of the UAVs, it can be noticed that all the UAVs have a SE above 1.6 bps/Hz starting from the 10th percentile, and regarding the GUEs, the most perceptible variation occurs around the 50th percentile, in which the red continous curve has an SE approximely 0.45 bps/Hz lower than the base scenario.

For the second case, consider that instead of 5 UAVs, 5 GUEs are added to the system, thus generating the green continous curve as the SE for all users. In the case of the GUEs, adding 5 more users is equivalent to double the system load, which as expected, descreases the SE through all the ECDF and, similarly to the previous case, the most noticeable variation happens on the vicinity of the 50th percentile, in which the green curve presents an SE roughly 1 bps/Hz lower than the case with only 5 GUEs. Futhermore, based on our analysis of the two cases of users arrival, it can be concluded that is more stressful for the system to increase the number of GUEs than the number of UAVs, by the same quantity.

Additionally, the yellow dotted line represents the case in which only UAVs are served in the network, resulting in a UE load of 10 UAVs. Observe that having 10 UAVs is the same as changing 5 GUEs to 5 UAVs in the first arrival case. Now, comparing the yellow dotted curve with red dotted one, it can be seen an overall improvement in the UAVs SE, indicating that UAVs interfere less among themselves.

B. Evaluation of Case Study 2

Now let us consider the following question: *Would performance improve if we set up two separate independent networks for GUEs and UAVs, by dividing the available frequency bandwidth into two equally orthogonal sub-bands?*

In other words, we are considering the impact of adopting a radio resource management policy that segregates the available sub-carriers depending on the UE type, not unlike a network slicing that divides radio resources to different types of services.

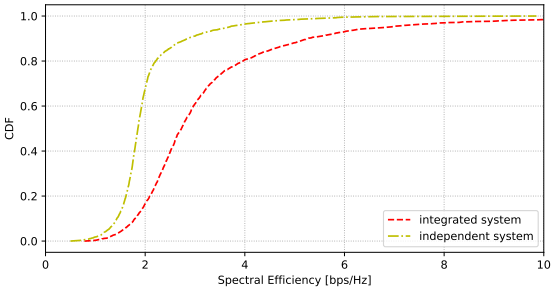

Fig. 3. Per-UE SE curves for both systems.

The Fig. 3 presents a comparison between two systems with 5 GUEs and 5 UAVs and with the same total bandwidth, both following the parameters on Table I. The so called integrated system is the one in which a single band is shared by all UEs irrespective of its category (the same system configuration of the previous sub-section). The independent system configuration is the one in which the same total bandwidth is split into two equal bandwidth parts of equal size. The channel estimation in both systems occurs without pilot contamination.

As it can be seen in Fig. 3 the integrated system outperforms the independent one in terms of per-UE SE, even for UEs in poor SINR conditions (on or below the curve's 10-th percentile). The integrated system is surely under more strain from increased co-channel interference, but the outstanding interference management capabilities of user-centric D-MIMO is able to supress its deleterious effects, rendering the coexistence of GUEs and UAVs in the same frequency resources seamless to the network operator. Additionaly, the L-MMSE combiner is optimal considering a distributed operation.

At last, taking the result exhibited on Fig. 3 and our analysis in consideration, it can be concluded that in order to provide better QoS while assuring a superior use of the network resources, namely a better SE, advanced interference mitigation techniques tend to yield a more decisive role than simply isolate the users in different orthogonal radio resources.

C. Evaluation of Case Study 3

The simulation parameters summarized in Table II were used for the remaining simulation results, in which a larger network is considered. Our objective in this subsection is to evaluate the performance of DCC for different channel gain threshold values.

The DCC technique is an effective clustering method to a cell-free network that yields SE values close to all APs transmission [5]. This conclusion was verified in our GUE/UAV mixed scenario as well, as it can be observed in Figure 4, in which the worst case SE penalty from restricting the cluster

TABLE II
SIMULATION PARAMETERS.

Parameter	Value
Coverage Area	1000x1000 m
Number of APs	$L = 100$
Tilt angle	$\theta_{\text{tilt}} = 5°$
Number of Sectors per AP	$S = 3$
Number of users	$K = 20$
UAV percentage	20%
Carrier frequency	f_c = 2 GHz
Communication bandwidth	W = 20 MHz
GUE and AP heights	1.5 m, 11.5 m
UAV height	uniform, $[23, 230]$ m
Uplink (UL) power per UE	p_k = 100 mW
Antenna spacing	$d = (1/2)\,\lambda$
GUEs σ_{sh} (LoS, NLoS)	4, 8.2 dB
UAVs σ_{sh} (LoS [11], NLoS)	$\max(2, 5e^{h_{\text{UAV}}/100})$, 8 dB
LoS probability model (GUEs,UAVs)	[10],[11]

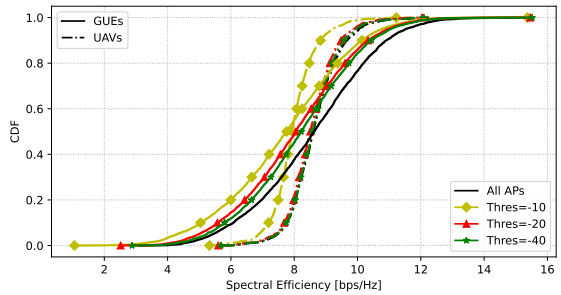

Fig. 4. SE curves varying cluster threshold.

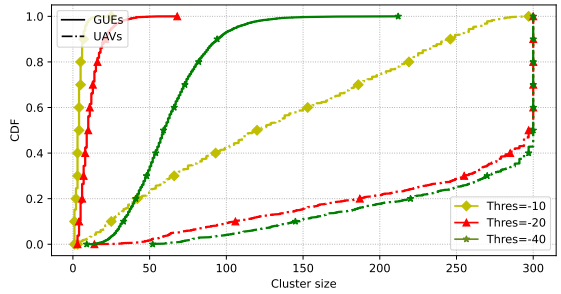

Fig. 5. Cluster size curves varying cluster threshold.

size is in the order of 16.6% and 7.6% at the 10-th percentile level for GUEs and UAVs, respectively.

Regarding the distribution of the cluster size itself, Figure 5 shows that UAV clusters are much larger, a result expected from its generally better path-gain under LoS. The UAVs' larger cluster sizes explain their smaller SE penalties in Figure 4. On the other hand, if an explicit cluster size restriction is imposed to all UEs (irrespective of its type), UAVs would be more penalized. This can be inferred by fixing a cluster size in the x-axis of Figure 5 and looking into the respective percentile of UEs experimenting such scenario. For instance, considering a threshold of -10 dB, by imposing a maximum cluster size of 50, about 70% of UAVs would be affected while no GUE would be impacted at all.

V. CONCLUSION

In this work, we studied how a user-centric D-MIMO network performs when UAVs and GUEs co-exist. Aspects considered in this work included the impact of adding UAVs to a GUE-only scenario, performance for varying UAV/GUE mixes and for different AP clustering approaches.

Our results show that, due to the outstanding interference management capabilities of D-MIMO technology, the negative impact that the increase in UAV load has on the network performance is no greater (actually smaller) than the corresponding impact that an equal increase in GUE load would have. Our results also show that on the subject of clustering, the large distinction between the UAVs and GUEs propagation properties suggests that a clustering scheme must address this difference to provide fair treatment for both UE types. Otherwise, UAVs will always get much larger AP clusters, yielding an imbalanced SE distribution and making UAVs more sensitive to explicit cluster size restrictions.

The perspectives for future works starts with the understanding that D-MIMO cellular networks can cope well with UAVs in terms of its interference management capabilities. The case in which cluster size is limited by network practical limitations should be further investigated in the case of UAVs from both a performance as well as a scalability perspective. Then a focus on mobility management is warranted as the potential high speeds and 3D mobility patters of UAVs are vastly different from traditional smartphone-based GUEs. Solutions using advanced artificial intelligence and machine learning for both mobility management and dynamic cluster formation are a promising research line to be pursued.

REFERENCES

[1] Z. Zhang, Y. Xiao, Z. Ma, *et al.*, "6G Wireless Networks: Vision, Requirements, Architecture, and Key Technologies," vol. 14, no. 3, pp. 28–41, 2019.

[2] D. G. S. Pivoto, T. T. Rezende, M. S. P. Facina, *et al.*, "A detailed relevance analysis of enabling technologies for 6g architectures," *IEEE Access*, vol. 11, pp. 89 644–89 684, 2023.

[3] Ö. T. Demir, E. Björnson, and L. Sanguinetti, "Foundations of user-centric cell-free massive MIMO," *Foundations and Trends in Signal Processing*, vol. 14, no. 3-4, pp. 162–472, 2021.

[4] M. Freitas, D. Souza, G. Borges, *et al.*, "Matched-decision ap selection for user-centric cell-free massive mimo networks," *IEEE Transactions on Vehicular Technology*, vol. 72, no. 5, pp. 6375–6391, 2023.

[5] E. Björnson and L. Sanguinetti, "Scalable cell-free massive MIMO systems," vol. 68, no. 7, pp. 4247–4261, Jul. 2020.

[6] J. Stanczak, I. Z. Kovacs, D. Koziol, J. Wigard, R. Amorim, and H. Nguyen, "Mobility challenges for unmanned aerial vehicles connected to cellular LTE networks," in *2018 IEEE 87th Vehicular Technology Conference (VTC Spring)*, 2018, pp. 1–5.

[7] G. Geraci, A. Garcia-Rodriguez, M. M. Azari, *et al.*, "What will the future of uav cellular communications be? a flight from 5g to 6g," *IEEE Communications Surveys & Tutorials*, vol. 24, no. 3, pp. 1304–1335, 2022.

[8] E. Björnson and E. Jorswieck, *Optimal Resource Allocation in Coordinated Multi-Cell Systems*. NOW Publishing, 2013.

[9] E. Björnson, J. Hoydis, and L. Sanguinetti, *Massive MIMO Networks: Spectral, Energy, and Hardware Efficiency*. NOW Publishing, 2017.

[10] 3GPP, *TR 38.901: Study on channel model for frequencies from 0.5 to 100 GHz*, Release 15, report, 2019.

[11] 3GPP, "Enhanced LTE support for aerial vehicles," 3rd Generation Partnerhsip Project, TR 36.777, Jan. 2018, v.15.0.0.

[12] ITU-R, "Guidelines for evaluation of radio interface technologies for IMT-advanced," International Telecommunications Union - Radiocommunications Sector (ITU-R), Tech. Rep., Dec. 2009.

[13] E. Björnson and L. Sanguinetti, "Making cell-free massive MIMO competitive with MMSE processing and centralized implementation," *IEEE Trans. Wireless Commun.*, vol. 19, no. 1, pp. 77–90, Sep. 2019.

[14] E. Björnson and L. Sanguinetti, "Making cell-free massive MIMO competitive with MMSE processing and centralized implementation," *IEEE Transactions on Wireless Communications*, vol. 19, no. 1, pp. 77–90, 2020.